

88  
RAIN CORE STRUCTURE STATISTICS DERIVED FROM RADAR AND DISDROMETER  
MEASUREMENTS IN THE MID-ATLANTIC COAST OF THE U.S.

Julius Goldhirsh, Bert H. Musiani

The Johns Hopkins University, Applied Physics Laboratory, Johns Hopkins  
Road, Laurel, MD 20707

**Abstract**

During a period spanning more than 5 years, low elevation radar measurements (PPIs) of rain were systematically obtained in the mid-Atlantic coast of the United States. Drop size distribution measurements with a nearby disdrometer were also acquired during the same rain days. The drop size data were utilized to convert the radar reflectivity factors to estimated rain rates for the respective rain days of operation. Employing high level algorithms to the radar data, core values of rain intensities were identified (peak rainrates), and families of rainrate isopleths were analyzed. In particular, equi-circle diameters of the family of isopleths enveloping peak rain intensities were statistically characterized. The results presented herein represents the analysis (ongoing) of two rain days, 12 radar scans, corresponding to 430 culled rain rate isopleths from an available data base of 22000 contours, approximately 100 scans encompassing 17 rain days. The results presented show trends of the average rain rate versus contour scale dimensions, and cumulative distributions of rain cell dimensions which belong to core families of precipitation.

**1. Introduction**

The statistics associated with the structure and spacing of rain cells are important to communicators interested in modeling rain attenuation for earth-satellite and terrestrial communications [CCIR, 1986]. Such statistics enable the evaluation of fade margin requirements for both single site and space diversity configurations [Goldhirsh, 1982]. A number of investigators have previously defined rain cell structures in different ways. For example, Crane [1983] characterized a cell as the 3 dB down isopleth of a core value of reflectivity factor. He subsequently related the corresponding area to the area averaged rain rate. Lopez et. al [1984] defined rain cell area by the minimum rain rate contour separating two cores. For the isolated cell case, only the minimum detectable contour values were considered. Konrad [1978] characterized cell areas by the 10 dB down contours from the peak value where the area statistics were equally weighted independent of core values. In addition to the above, this effort differs from previous ones in the following ways: (1) The radar employed has a resolution significantly larger than those used by the other investigators (with the exception of Konrad [1978]), and (2) the previous results were generally expressed in terms of radar reflectivity factors or in terms of rainrates employing fixed empirical relations. This effort incorporated the results of drop size distribution measurements used to convert reflectivity factors to rainrates.

We extend a previous work by Goldhirsh and Musiani [1986] in which 22000 rate isopleths were generated from 100 low elevation azimuthal radar scans and disdrometer measurements encompassing 17 rain days. The radar measurements were made with the high power, high resolution SPANDAR radar at the NASA Wallops Flight Facility, Wallops Island, Virginia. In the previous analysis, the areas of the rainrate isopleths were calculated, and the probability densities and cumulative distributions associated with the equi-circle diameters of the rain rate isopleths were determined; an equi-circle diameter being defined as the diameter of a circle whose area equals the contour area. The previous analysis by the authors did not relate the cell dimensions to "core" rain or "peak" rain intensity levels of rain cells as we do here, but categorized the isopleths according to rainrate levels independently of whether it belonged to high or low core values.

## 2. Experimental Aspects

### 2.1 Radar Measurements

The nominal operating parameters of the SPANDAR radar are given in Table 1. Radar measurements of the rain structure were made over contiguous gates of 150 m in range within an annular region from 10 to 100 km from the radar. At a fixed elevation of  $0.4^\circ$ , the azimuthal scan rate was  $3^\circ/\text{s}$ , and a set of radar measurements in range was obtained for approximately each  $1^\circ$  azimuthal interval. The absolute calibration uncertainty of the radar was approximately 1 dB. The power measurements were integrated in real time via an interfacing processor and stored on a 9 track tape recorder for off-line reduction and analysis.

### 2.2 Disdrometer Measurements

A Rowland disdrometer [1979] was employed to measure the family of drop size distributions during each rain day in which radar data were accumulated. The disdrometer system is an electromechanical sensor comprised of a piezoelectric crystal imbedded in a plexiglass block. The sensor was calibrated such that raindrops of known diameters falling at terminal velocity on the sensor head generated unique voltages at the output of the crystal. These voltages were fed through an analog to digital converter, stored on magnetic tape, and analysed. Scatter plots of rain rate  $R$  ( $\text{mm}/\text{h}$ ) versus radar reflectivity factor  $Z$  ( $\text{mm}^6/\text{m}^3$ ) were generated for each rain day where each point on the scatter plot represented the acquisition of 1000 rain drops from which a single calculation was made of  $R$  and  $Z$ . Typically, scatter plots consisted of more than 100 distributions and sampling periods ranged from one to two hours. Least square  $R - Z$  relations were calculated having the form  $R = a Z^b$  from which values of  $a$  and  $b$  were generated for each rain day.

In Table 2 is a listing of these disdrometer least square fit power relations for each of the 17 rain days in which disdrometer data were acquired. The rainrate standard errors were found to range between 14% and 40% with an overall average of 24%. The radar measured reflectivities for each of the rain days were converted to rainrates employing the best fit values  $a$  and  $b$  in Table 2. These relationships are plotted in Figure 1 as a demonstration of the variability of the  $R-Z$  relations in the mid-Atlantic

coast geographic region over which the measurements were made. We note that at  $Z = 10^3 \text{ mm}^6/\text{m}^3$ , the span of rain rates range from  $R \approx 1.5$  to  $4 \text{ mm/h}$ . At  $Z = 10^5 \text{ mm}^6/\text{m}^3$ ,  $R$  ranges from 40 to  $100 \text{ mm/h}$ . It is interesting to note that the  $R$ - $Z$  relation of Marshall-Palmer [1949] given by  $R \approx .0365 Z^{0.625}$  is bounded by the family of distributions in Figure 1 and results in  $R = 2.7$  and  $48.7 \text{ mm/h}$  at  $Z = 10^3$  and  $10^5 \text{ mm}^6/\text{m}^3$ , respectively.

### 3. Contour Levels

#### 3.1 Method of Construction

As mentioned, a set of reflectivity levels were originally determined for approximately every  $1^\circ$  in azimuth and 150 m in range. To mitigate the effects of noisy data, the reflectivity factors over three range bins were averaged. As mentioned, they were converted to rain rates using the measured relationships given in Table 2. The corresponding rain rates were subsequently mapped onto an X-Y grid indicating the east-west and north-south distance locations relative to the SPANDAR radar. They were then binned over rainrate intervals defined by the "Level Numbers (LN)" in Table 3. An algorithm was implemented which did the following: (a) identified contiguous values of LN, (b) connected a line between the contiguous values of LN, and (c) recognized when the line closed upon itself to establish a closed contour.

A second algorithm was developed which identified clusters of rain rate isopleths which enveloped "core" rainrates. Those isopleths which identified the same core value were grouped into a family of contours and are referred to as a "core family". For each isopleth belonging to a core family, the area, centroid location, maximum and minimum lengths from the centroid to each respective contour, and core orientation (angles relative to north in which the maximum and minimum lengths are directed) were determined. The core family characteristics were then grouped in terms of their core levels (peak rainrates) for statistical analysis. As an example, we show in Figure 2 a complex set contours in the south-west quadrant belonging to core families whose exterior are at levels 5 and greater. These contours were derived from radar measurements made on February 17, 1983. In Figure 3, we have zoomed in on a family of contours associated with the core level  $LN = 9$  ( $32 - 43 \text{ mm/h}$ ) whose core centroid is located at approximately  $X = -43.5 \text{ km}$ ,  $Y = -28.5 \text{ km}$  relative to the radar (see arrow in Figure 2).

#### 3.2 Data Base

In Table 4 are summarized the data bases available for analysis. The data covers an approximate five and one half year period encompassing 17 rain days and all seasons. Approximately 100 scans (PPIs) are available for analysis over which more than 22000 closed contours require culling. As of this writing, the statistics associated with 430 culled contours have been reduced and analyzed. These data encompass the rain days January 2, 1979 and February 17, 1983 and correspond to 12 radar scans. The effort is continuing with the goal to analyze the full data base.

#### 4. Results

In Figure 4 are shown conditional cumulative distributions for a family of contours corresponding to the peak rain rate for LN = 7. These statistics address the question, "Given rain rate isopleths belonging to a core value of LN = 7 (18 - 24 mm/h), what is the probability that the isopleths have equi-circle diameters which exceed given values?" Only contours of level 5 and greater are considered in this analysis due to excessive computer times at the smaller levels. Furthermore, only contours with rainrates which monotonically increase (or are constant) within each contour were considered in the determination of the statistics. We note (Figure 4) that the distributions have approximate exponential shapes for diameters greater than 1 km. Families of distributions have also been determined for core levels 8 and 9 (not shown) showing similar exponential decrease in probability with increasing diameter. In Figure 5 is shown a family of curves depicting the average equi-circle diameters (ordinates) for core level numbers ranging from 7 to 11. The abscissa represents the center rainrates in the intervals defined in Table 3.

#### 5. Summary and Conclusions

The results presented herein provide rain cell structure information for modelers of slant path attenuation interested in the attenuation effects of precipitation for earth-satellite or terrestrial communication configurations operating at frequencies above 10 GHz. The developed algorithms enable the grouping of families of rainrate isopleths belonging to core values of rain intensities. Preliminary analyses for two rain days show well defined trends in the contour diameter cumulative distributions and average equi-cell diameter variations with rainrate. It is observed in Figure 5 that core rainrates with greater intensities contain significantly more structure and larger cell diameters than cells having lower core rainrates. The overall average equi-circle diameter for each core family with good approximation linearly decreases with increasing rainrate over the indicated range of values. For diameters greater than 1 km, the cumulative probability distributions of contour diameters exponentially reduce with increasing diameter (Figure 4). The exponential decay in the cumulative distributions is consistent with the cell results of Goldhirsh and Musiani [1979] for the combined cell diameter case.

#### 6. Acknowledgements

The authors are grateful Norman Gebo, Norris Beasley and George Bishop for assisting in acquiring the radar and disdrometer data base at the NASA Wallops Flight Facility at Wallops Island, VA. This work was supported by the Communications Division of NASA Headquarters under contract to APL # N00039-89-C-5301.

#### References

CCIR (International Radio Consultative Committee), "Recommendations and Reports of the CCIR, 1986", Propagation in Non-Ionized Media, Vol V, XVIth Plenary Assembly, Dubrovnik, 1986.

Crane, R. K, "An Analysis of Radar Data to Obtain Storm Cell Sizes, Shapes and Spacings, Thayer School of Engineering, Dartmouth College, Hanover, NH, Tech Rep, Apr., 1983.

Goldhirsh, J., "Space Diversity Performance Prediction for Earth-Satellite Paths Using Radar Modeling Techniques", Radio Science, Vol 17, No. 6, pp 1400-1410, Nov-Dec, 1982.

Goldhirsh, J., and B. Musiani, "Rain Cell Size Statistics Derived from Radar Observations at Wallops Island, Virginia", IEEE Transactions on Geoscience and Remote Sensing, Vol GE-24, No. 6, November, pp 947 - 954, 1986.

Konrad, T. G., "Statistical Models of Summer Rainshowers Derived from Fine Scale Radar Observations", J. Applied Meteorology, Vol 17, No 2, pp 171 - 188, Feb., 1978

Lopez, R. E., D. O. Blanchard, D. Rosenfield, W. L. Hiscox and M. J. Casey, "Population Characteristics, Development Processes and Structure of Radar Echoes in South Florida", Monthly Weather Rev., Vol 112, pp 56 - 75, Jan., 1984.

Marshall, J. S. and W. McK. Palmer, "The Distribution of Raindrops with Size", J. Meteorology, Vol 6, pp 243-248, 1949.

Rowland, J. R., "Comparison of Two Different Raindrop Disdrometers", Proc. 17th Radar Meteor. Conf., Seattle, WA, Oct. 26-29, pp398-405, 1979.

Table 1  
Nominal Radar Parameters for SPANDAR

Radar Location	Lat - $37^{\circ} 51' 16.8''$ N Long - $75^{\circ} 30' 48.4''$ W
Radar Name	SPANDAR (FPS 18)
Peak Power	1 megawatt
Center Frequency	2.84 GHz
Diameter of Dish	18.3 m
Gain	50.6 dB
Beamwidth	$0.4^{\circ}$
Pulse Width	1 $\mu$ sec
Range Resolution	150 m
Prf	320 Hz
Freq Diversity:	
# of Steps	24
Step Size	> 11 MHz
Polarization	Vertical
# of Samples	128
Sampling Time	0.4 sec
# of Gates	871
Calib Error	+/- 1 dB

**Table 2**  
 Listing of Disdrometer Derived Best Fit  $R = aZ^b$   
 Parameters where  $[R] = \text{mm/h}$  and  $[Z] = \text{mm}^6/\text{m}^3$   
 (Julian days indicated in parentheses)

Day	a	b	% SE
6/6/77 (157)	$7.03 \times 10^{-3}$	0.812	24.6
6/9/77 (160)	$6.20 \times 10^{-2}$	0.566	24.8
8/24-25/77 (236)	$9.73 \times 10^{-3}$	0.780	29.0
9/14/77 (257)	$3.68 \times 10^{-2}$	0.655	17.8
11/27/78 (331)	$5.71 \times 10^{-2}$	0.572	29.8
1/2/79 (002)	$4.0 \times 10^{-3}$	0.86	30.0
1/24/79 (024)	$4.52 \times 10^{-2}$	0.644	26.1
3/6/79 (065)	$1.90 \times 10^{-2}$	0.751	39.7
4/4/79 (094)	$3.15 \times 10^{-2}$	0.676	18.9
5/31/79 (151)	$7.86 \times 10^{-3}$	0.767	19.8
6/11/79 (162)	$3.26 \times 10^{-2}$	0.615	22.9
9/5/79 (248)	$7.235 \times 10^{-3}$	0.796	--
3/14/80 (073)	$7.41 \times 10^{-2}$	0.566	24.1
4/10/80 (100)	$1.79 \times 10^{-2}$	0.674	28.5
4/15/80 (105)	$3.85 \times 10^{-2}$	0.604	14.2
11/15/83 (319)	$1.65 \times 10^{-2}$	0.739	17.4
2/17/83 (048)	$3.6 \times 10^{-2}$	0.625	19.4

**Table 3**  
 Contour Level Numbers (LN),  
 Corresponding Rainrate  
 and Nominal (MP) dBZ Intervals

Contour Level #	Rain Rate Interval (mm/hr)	Nominal dBZ Interval
0	>.5	>18
1	0.5-1	18-23
2	1-2	23-28
3	2-4	28-33
4	4-8	33-37
5	8-12	37-40
6	12-18	40-43
7	18-24	43-45
8	24-32	45-47
9	32-42	47-49
10	42-56	49-51
11	56-75	51-53
12	75-100	53-55
13	100-133	55-57
14	133-205	57-60
15	>205	>60

**Table 4**  
 Data Base Available for Analysis

Number of Rain Days	17
Winter	6
Spring	6
Summer	3
Fall	2
Number of Scans (PPIs)	96
Number of Total Contour	22,308

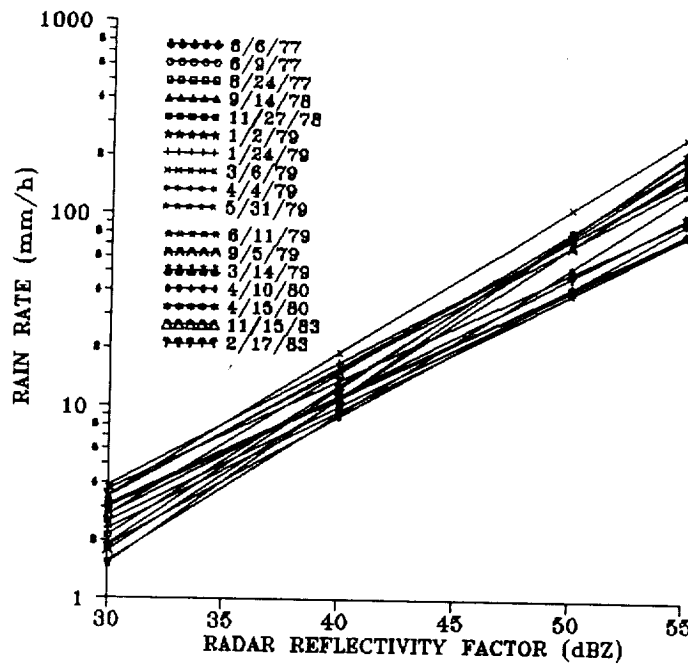


Figure 1 Family of disdrometer derived R-Z relations where each curve represents a different rain day (Table 2).

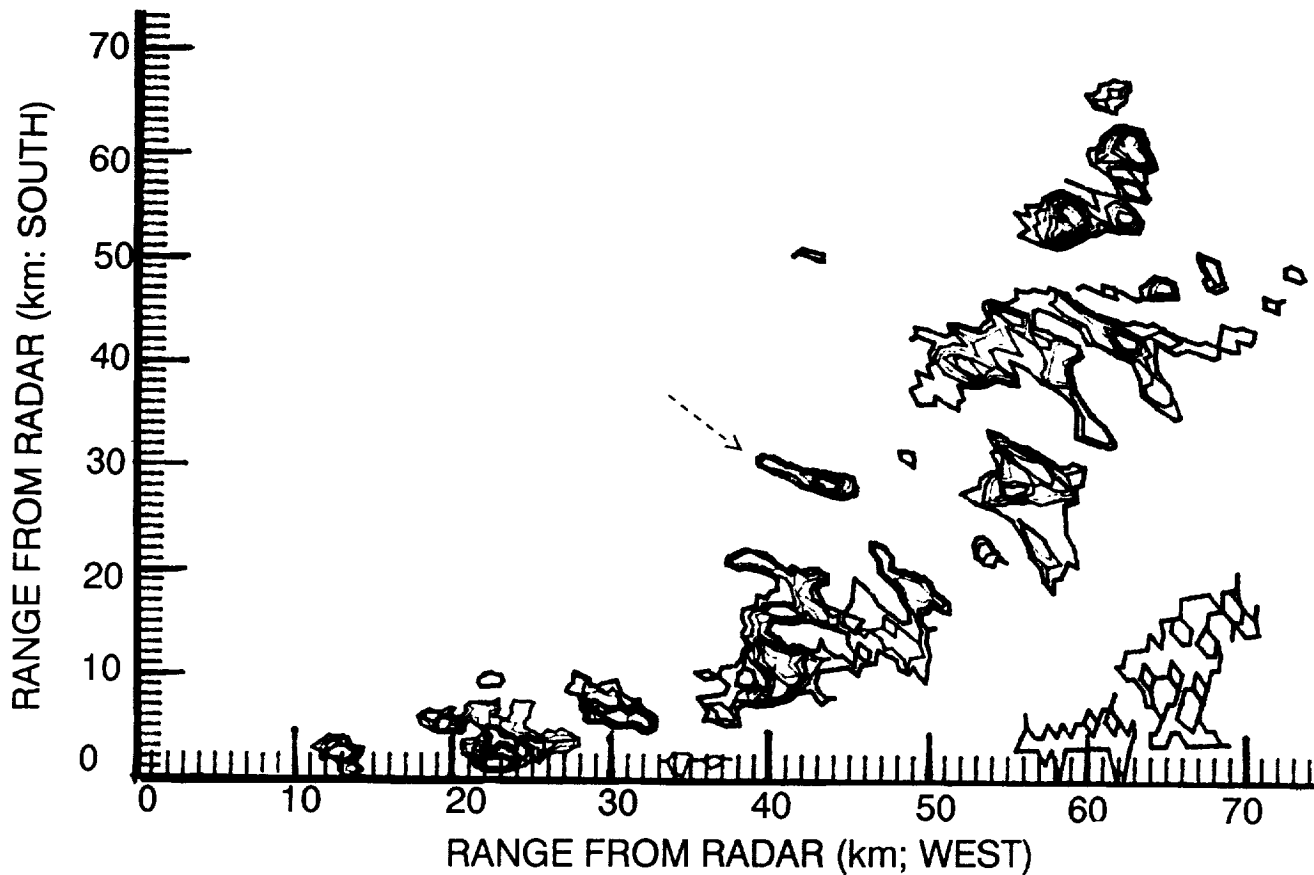


Figure 2 Rainrate isopleths belonging to core cells in the southwest quadrant of a radar scan on February 17, 1983. Exterior isopleths are level 5 or greater.

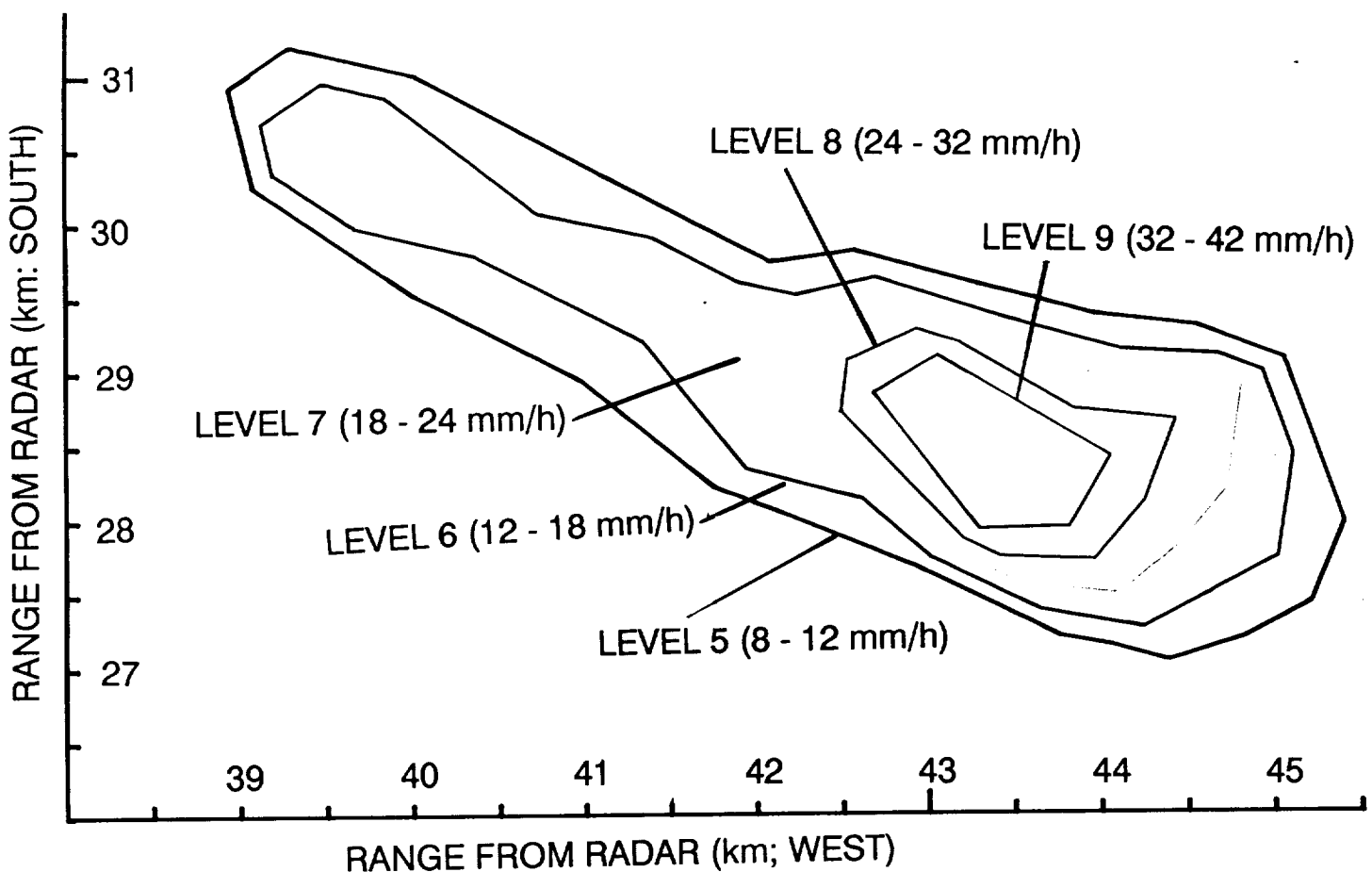


Figure 3 Zoomed in contour family of isopleths belonging to the core cell  $LN = 9$  at  $X = -43.5$  km,  $Y = -28.5$  km (Figure 2).

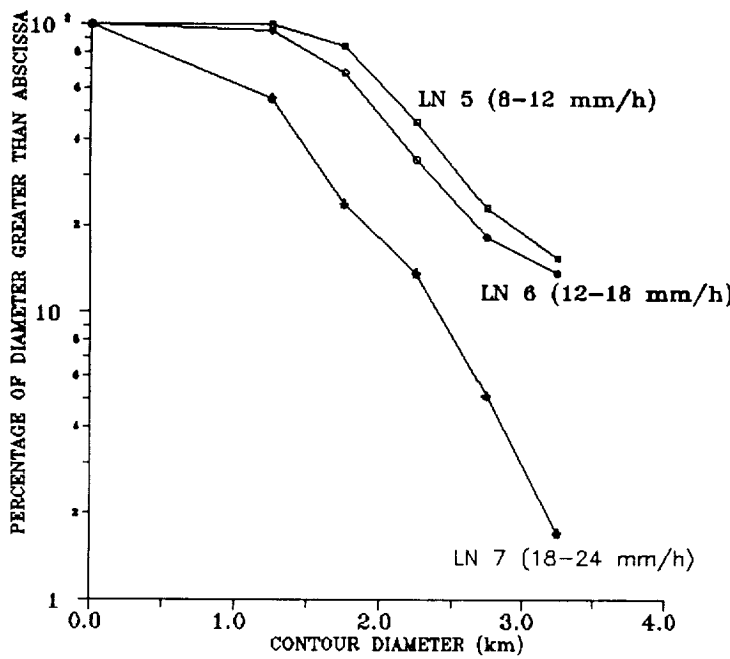


Figure 4  
Cumulative distributions for the isopleths belonging to the core family  $LN = 7$ .

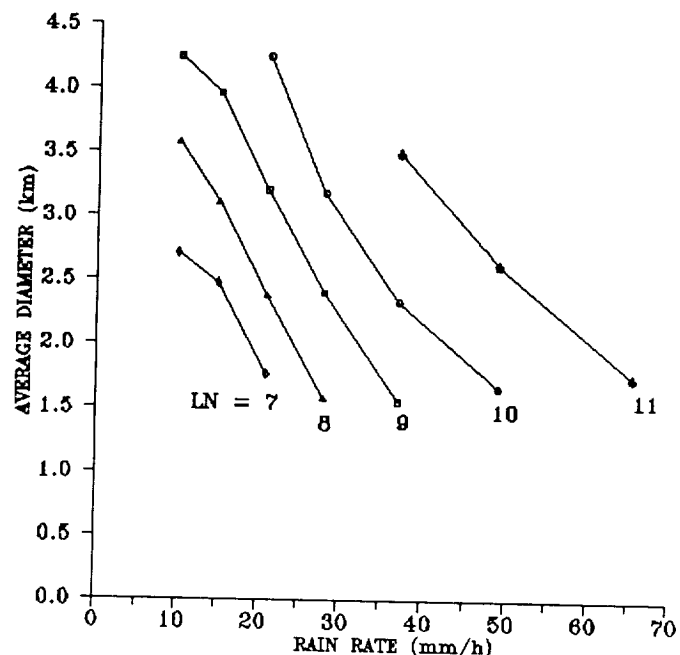


Figure 5  
Average diameter versus center rainrates for core families in the level range  $LN = 7$  to 11 (Table 3).